Acta Crystallographica Section D
Biological Crystallography
ISSN 0907-4449

Crystallization and preliminary X-ray diffraction studies of D-glyceraldehyde-3-phosphate dehydrogenase from the hyperthermophilic archaeon *Methanothermus fervidus*

C. Charron,[a] F. Talfournier,[b] M. N. Isupov,[c] G. Branlant,[b] J. A. Littlechild,[c] B. Vitoux[a] and A. Aubry[a]*

[a]Laboratoire de Cristallographie et Modélisation des Matériaux Minéraux et Biologiques, UPRESA CNRS 7036, Université Henri Poincaré, Nancy I, BP 239, 54506 Vandoeuvre-lès-Nancy, France, [b]Maturation des ARN et Enzymologie Moléculaire, UMR CNRS 7567, Université Henri Poincaré, Nancy I, BP 239, 54506 Vandoeuvre-lès-Nancy, France, and [c]Schools of Chemistry and Biological Sciences, University of Exeter, Stocker Road, Exeter EX4 4QD, England

Correspondence e-mail: aubry@lcm3b.u-nancy.fr

Received 29 January 1999
Accepted 26 April 1999

PDB Reference: D-glyceraldehyde-3-phosphate dehydrogenase, 1cf2.

The homotetrameric holo-D-glyceraldehyde-3-phosphate dehydrogenase from the hyperthermophilic archaeon *Methanothermus fervidus* has been crystallized in the presence of $NADP^+$ using the hanging-drop vapour-diffusion method. Crystals grew from a solution containing 2-methyl-2,4-pentanediol and magnesium acetate. A native data set has been collected to 2.1 Å using synchrotron radiation and cryocooling. Diffraction data have been processed in the orthorhombic system (space group $P2_12_12$) with unit-cell dimensions a = 136.7, b = 153.3, c = 74.9 Å and one tetramer per asymmetric unit.

1. Introduction

The phosphorylating D-glyceraldehyde-3-phosphate dehydrogenase (GAPDH) catalyses the reversible oxidation of D-glyceraldehyde-3-phosphate to 1,3-diphosphoglycerate and requires nicotinamide adenine dinucleotide $NAD(P)^+$ as an obligatory cofactor (Harris & Waters, 1976). GAPDH enzymes (E.C. 1.2.1.12) extracted from eubacterial and eukaryotic sources are usually NAD^+-dependent, while archaeal GAPDHs exhibit dual cofactor specificity with a marked preference for $NADP^+$ (Fabry & Hensel, 1987; Jones *et al.*, 1995; Zwickl *et al.*, 1990). With the exception of the chloroplastic enzymes, all phosphorylating GAPDHs known so far contain four identical subunits with a monomeric M_r of ~36 kDa. Primary structure alignments (Fabry *et al.*, 1989; Zwickl *et al.*, 1990; Arcari *et al.*, 1993; Talfournier *et al.*, 1998) reveal significant levels of identity between archaeal GAPDHs, but more speculative amino-acid sequence comparisons including eukaryotic and eubacterial GAPDHs (Fabry & Hensel, 1988; Fabry *et al.*, 1989) do not provide evidence for a unique three-dimensional fold common to all GAPDHs.

Crystal structures have been solved for GAPDH enzymes isolated from a number of eukaryotic and eubacterial species including american lobster (Moras *et al.*, 1975), chinese lobster (Song *et al.*, 1998), man (Watson *et al.*, 1972), parasites such as *Trypanosoma brucei* (Vellieux *et al.*, 1993) and *Leishmania mexicana* (Kim *et al.*, 1995), eubacteria such as mesophilic *Escherichia coli* (Duée *et al.*, 1996) and *Bacillus coagulans* (Griffith *et al.*, 1983), moderately thermophilic *B. stearothermophilus* (Skarzynski *et al.*, 1987), thermophilic *Thermus aquaticus* (Tanner *et al.*, 1996) and hyperthermophilic *Thermotoga maritima* (Korndörfer *et al.*, 1995). Crystallization and preliminary X-ray results have recently been described for GAPDH from the hyperthermophilic archaeon *Sulfolobus solfataricus* (Fleming *et al.*, 1998).

The archaeon *Methanothermus fervidus* lives in extreme conditions and grows optimally at 358 K. Thus, the determination of the three-dimensional structure of GAPDH isolated from this hyperthermophilic microorganism will constitute a significant contribution to the knowledge of the structural determinants responsible for molecular and cellular thermostability.

2. Materials and methods

2.1. Purification

The wild-type recombinant GAPDH from *M. fervidus* was genetically overexpressed in *E. coli* HB101 cells and purified to homogeneity by the procedure described by Talfournier *et al.* (1998). Protein solutions (10 mg ml^{-1}) were prepared in 10 m*M* Tris–HCl buffer (pH 7.5) containing 1 m*M* dithiothreitol and 2 m*M* EDTA.

2.2. Crystallization

Screening for optimal crystallization conditions was performed using the hanging-drop method of vapour diffusion and the sparse-matrix factorial search of Jancarik & Kim (1991). Screening was carried out at three different temperatures, namely 277, 285 and 293 K. For each experiment, 4 µl of the GAPDH solution was mixed with an equal volume of a reservoir solution.

2.3. Diffraction measurements

X-ray diffraction intensity data were collected at the European Synchrotron Radiation Facility (ESRF) at Grenoble (France). Prior to data collection, a suitable native crystal was soaked in a cryobuffer identical to the mother liquor but with the 2-methyl-2,4-pentanediol concentration increased to 20%. The crystal was then flash-cooled in a nitrogen-gas stream at 100 K before mounting. The wavelength of the incident radiation was 0.987 Å and the crystal-to-detector distance was 245 mm. The diffraction spots were recorded on a Princeton CCD camera (1242 × 1152 pixels) with a 0.5° oscillation for each CCD image; a total range of 135° was covered. Data were processed using the *MARXDS* package (Klein, 1993; Kabsch, 1993).

A second set of X-ray data was collected in our laboratory at 100 K on a DIP2030 Enraf–Nonius area detector using a rotating-anode generator. The wavelength of the incident radiation was 1.542 Å and the crystal-to-detector distance was 200 mm. A total range of 110° was covered, with 1.0° oscillation per image. Data were processed using *DENZO* (Otwinowski & Minor, 1996).

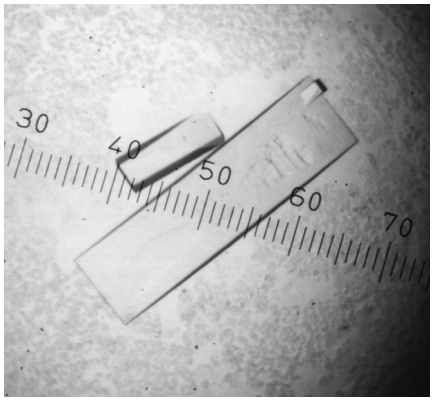

Figure 1
Crystals of recombinant *M. fervidus* GAPDH grown in 2-methyl-2,4-pentanediol, magnesium acetate and cacodylate buffer as described in the text (ten graduations = 0.25 mm).

3. Results and discussion

Large crystals suitable for X-ray diffraction analysis (Fig. 1) were obtained under experimental conditions consisting of 18%(*v*/*v*) 2-methyl-2,4-pentanediol, 12 m*M* magnesium acetate, 2 m*M* EDTA, 1 m*M* dithiothreitol, 60 m*M* cacodylate buffer (pH 6.5) at 285 K.

A total of 415252 reflections in the resolution range 35–2.1 Å were collected at the synchrotron beamline. They were reduced to 82965 unique reflections. Overall, the data set had an $R_{\rm sym}$ of 5.6% on intensities ($R_{\rm sym} = \sum|I - \langle I\rangle|/\sum I$) and was 91.7% complete (Table 1). We observed a low completeness at low resolution [67.9% in the resolution range 15.0–8.0 Å; $I/\sigma(I)$ = 15.5, $R_{\rm sym}$ = 4.0%] which was because of overloading.

Autoindexing routines gave solutions consistent with an orthorhombic space group, which enabled unit-cell dimensions to be refined to a = 136.7, b = 153.3, c = 74.9 Å. Systematic extinctions [$I/\sigma(I) < 3$] of $h00$ (with $h = 2n + 1$) and $0k0$ (with $k = 2n + 1$) reflections were observed, corresponding to the $P2_12_12$ space group. Both crystallization conditions and space group are different from those previously described by Fabry *et al.* (1988), who obtained crystals belonging to the tetragonal space group $P4_122$.

As biochemical data have reliably demonstrated that the *M. fervidus* GAPDH is composed of four identical subunits of 337 residues (Fabry & Hensel, 1987; Talfournier *et al.*, 1998), comparison of the unit-cell volume with that of holoenzyme crystals from *B. stearothermophilus* (Skarzynski *et al.*, 1987) suggested the presence of one tetramer of *M. fervidus* GAPDH per asymmetric unit. In good agreement with values known for other proteins (Matthews, 1968), the predicted packing density value V_m would then be 2.6 Å^3 Da^{-1} and the probable solvent content would be 47.3%.

On the basis of the molecular 222 symmetry systematically observed in all presently known three-dimensional structures of tetrameric GAPDHs, a self-rotation function was calculated using the *GLRF* program (Tong & Rossmann, 1990) in order to obtain the orientations of the three putative twofold non-crystallographic axes of the *M. fervidus* tetramer in the asymmetric unit. A stereographic projection (Fig. 2) revealed two peaks at Φ = 34, Ψ = 90° and Φ = 56, Ψ = 90° which corresponded to two non-crystallographic twofold axes. Assuming a 222 symmetry, the third molecular twofold axis then would lie parallel to crystallographic c axis.

Indeed, a native Patterson map (w = 0 section) indicated a high-intensity peak characteristic of a non-crystallographic twofold axis and a crystallographic twofold axis parallel to each other (Fig. 3). The location of this peak revealed the fractional

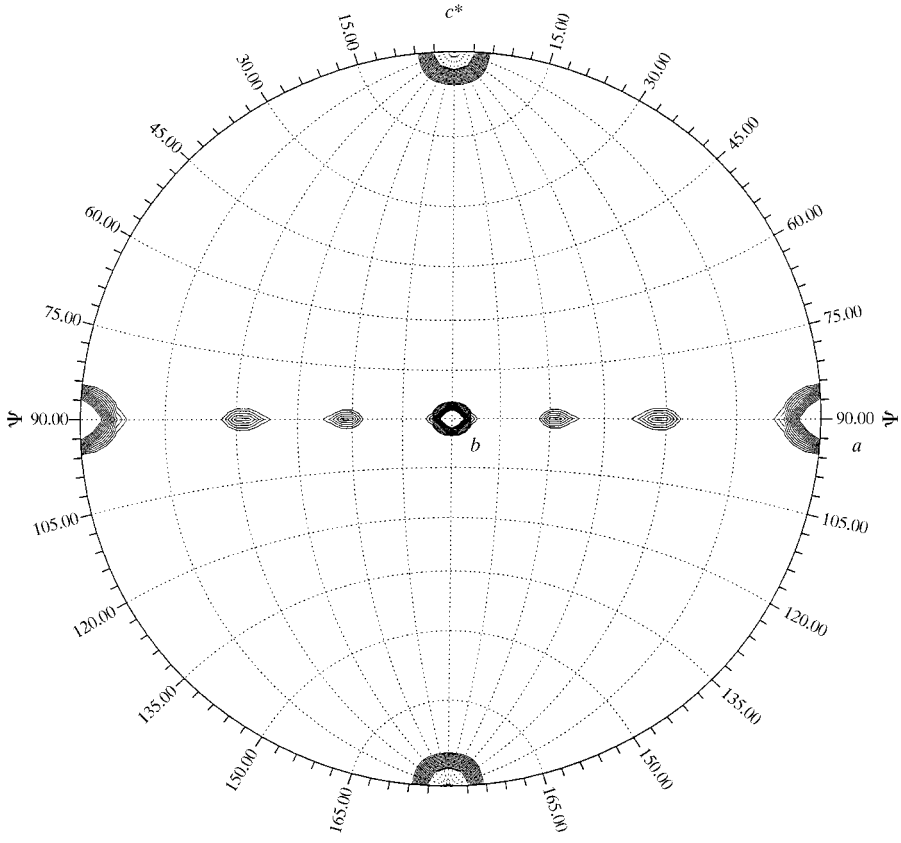

Figure 2
Stereographic projection of the $\kappa = 180°$ section of a self-rotation function showing the three non-crystallographic twofold axes. Data were included between 10.0 and 3.5 Å with a 25 Å integration radius. The low-level cutoff is 2σ with contour levels of 1σ.

Table 1
X-ray data measurement statistics.

	ESRF data	'In-house' data
Resolution limit (Å)	2.1	2.5
R_{sym} (overall) (%)	5.6	4.6
Completeness (overall) (%)	91.7	93.6
$I/\sigma(I)$ (overall)	9.1	18.0
Multiplicity (overall)	5.0	3.1
R_{sym} (last shell) (%)	15.1 (2.11–2.17 Å)	13.9 (2.50–2.59 Å)
Completeness (last shell) (%)	69.3	74.6
$I/\sigma(I)$ (last shell)	4.0	4.9

coordinates of the molecular axis relative to the crystal axis c: $x = 0.225$ and $y = 0.250$.

The recently solved three-dimensional structure of *S. solfataricus* GAPDH (Fleming *et al.*, 1998; J. A. Littlechild, personal communication), which shows 49% identity with the *M. fervidus* GAPDH, was tested as a model which was probably well adapted for molecular-replacement calculations; previous attempts using the native structures of eubacterial GAPDHs as models failed to converge toward a plausible three-dimensional structure for *M. fervidus* GAPDH.

The tetramer of *S. solfataricus* GAPDH was used as a model for molecular-replacement studies in the resolution range 10.0–4.0 Å using the program *AMoRe* (Navaza, 1987, 1994). To provide a sufficient amount of data at low resolution, the ESRF data were merged with the 'in-house' data with an R_{merge} of 8.9% in the resolution range 10–4 Å using the program *BLANC* (Vagin *et al.*, 1998). The rotation function calculated with a 23 Å integration radius had four peaks with height of 16 r.m.s. When the model was rotated using any of these solutions, one of its molecular dyads appeared to be parallel to the crystallographic twofold axis c, in agreement with the self-rotation function and the native Patterson map results.

Subsequently, the orientation corresponding to the first peak was used in the calculation of the translation function and gave two major peaks. One of them gave a correlation $C = \sum(|F_o| - \langle|F_o|\rangle)\,(|F_c| - \langle|F_c|\rangle) / [\sum(|F_o| - \langle|F_o|\rangle)^2 \sum(|F_c| - \langle|F_c|\rangle)^2]^{1/2}$ of 51.1% and an R factor $R = \sum \big||F_o| - |F_c|\big| / \sum |F_o|$ of 50.1%, while the next solution exhibited a correlation of 49.8% and an R factor of 50.8%. The third peak had a correlation of only 36.4%. However, neither of the two first solutions could be refined further, possibly owing to the relative movement of subunits within the tetramer. Thereafter, each subunit was tentatively taken as an independent rigid body and a refinement using *REFMAC* (Murshudov *et al.*, 1997) in the resolution range 10–4 Å was then performed in order to optimize the rotational and translational parameters corresponding to the first solution. The R factor fell to 47.0%.

Refinement then took place using the ESRF data in the resolution range 10–2.1 Å without NCS restraints using *REFMAC* (Murshudov *et al.*, 1997). 2% of the data were selected for R_{free} calculations. The model, which has now been refined to a final R factor of 19.4% and R_{free} of 25.7%, clearly appears to be of the holo type (one $NADP^+$ molecule per monomer) and will be described in detail elsewhere.

Structural analysis is now in progress with the aim of comparing the now available *S. solfataricus* (J. A. Littlechild, personal communication) and *M. fervidus* archaeal GAPDH crystal structures and of providing new insights into the rational description of the molecular phenomena responsible for extreme thermostability.

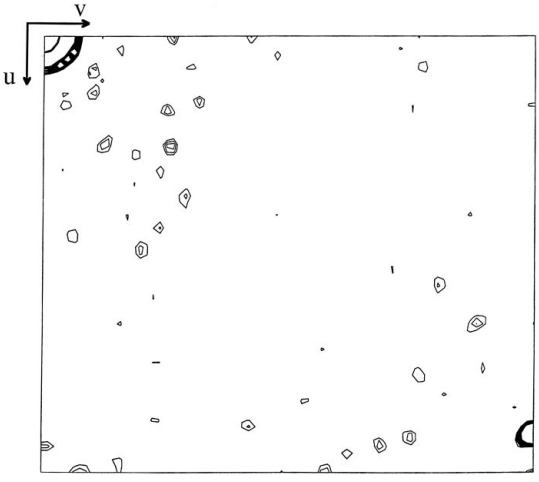

Figure 3
Section $w = 0$ of the native Patterson map (u from 0 to 1/2 and v from 0 to 1/2) showing a high peak (31σ), located at $u = 0.45$ and $v = 0.50$, which is related to non-crystallographic symmetry. Data were included in the resolution range 10.0–3.5 Å. The low-level cutoff is 1.5σ with contour levels of 0.5σ.

Comments and proposals from both reviewers were deeply appreciated.

References

Arcari, P., Dello Russo, A., Ianniciello, G., Gallo, M. & Bocchini, V. (1993). *Biochem. Genet.* **31**, 241–251.

Duée, E., Olivier-Deyris, L., Fanchon, E., Corbier, C., Branlant, G. & Dideberg, O. (1996). *J. Mol. Biol.* **257**, 814–838.

Fabry, S. & Hensel, R. (1987). *Eur. J. Biochem.* **165**, 147–155.

Fabry, S. & Hensel, R. (1988). *Gene*, **64**, 189–197.

Fabry, S., Lang, J., Niermann, T., Vingron, M. & Hensel, R. (1989). *Eur. J. Biochem.* **179**, 405–413.

Fabry, S., Lehmacher, A., Bode, W. & Hensel, R. (1988). *FEBS Lett.* **237**, 213–217.

Fleming, T. M., Jones, C. E., Piper, P. W., Cowan, D. A., Isupov, M. N. & Littlechild, J. A. (1998). *Acta Cryst.* D**54**, 671–674.

Griffith, J. B., Lee, B., Murdock, A. L. & Amelunxen, R. E. (1983). *J. Mol. Biol.* **169**, 963–974.

Harris, J. I. & Waters, M. (1976). *The Enzymes*, Vol. 13, edited by P. D. Boyer, pp. 1–49. New-York: Academic Press.

Jancarik, J. & Kim, S.-H. (1991). *J. Appl. Cryst.* **24**, 409–411.

Jones, C. E., Fleming, T. M., Cowan, D. A., Littlechild, J. A. & Piper, P. W. (1995). *Eur. J. Biochem.* **233**, 800–808.

Kabsch, W. (1993). *MARXDS, Version* 1.0 *Documentation.* MAR Research GMBH, D-22547 Hamburg, Germany.

Kim, H., Feil, I. K., Verlinde, C. L. M. J., Petra, P. H. & Hol, W. G. J. (1995). *Biochemistry*, **34**, 14975–14986.

Klein, C. (1993). *MARXDS MARSCALE Manual, Version* 1.4. MAR Research GMBH, D-22547 Hamburg, Germany.

Korndörfer, I., Steipe, B., Huber, R., Tomschy, A. & Jaenicke, R. (1995). *J. Mol. Biol.* **246**, 511–521.

Matthews, B. W. (1968). *J. Mol. Biol.* **33**, 491–497.

Moras, D., Olsen, K. W., Sabesan, M. N., Buehner, M., Ford, G. C. & Rossmann, M. G. (1975). *J. Biol. Chem.* **250**, 9137–9162.

Murshudov, G. N., Vagin, A. A. & Dodson, E. J. (1997). *Acta Cryst.* D**53**, 240–255.

Navaza, J. (1987). *Acta Cryst.* A**43**, 645–653.

Navaza, J. (1994). *Acta Cryst.* A**50**, 157–163.

Otwinowski, Z. & Minor, W. (1996). *Methods Enzymol.* **276**, 307–326.

Skarzynski, T., Moody, P. C. E. & Wonacott, J. A. (1987). *J. Mol. Biol.* **193**, 171–187.

Song, S., Li, J. & Lin, Z. (1998). *Acta Cryst.* D**54**, 558–569.

Talfournier, F., Colloc'h, N., Mornon, J.-P. & Branlant, G. (1998). *Eur. J. Biochem.* **252**, 447–457.

Tanner, J. J., Hecht, R. M. & Krause, K. L. (1996). *Biochemistry*, **35**, 2597–2609.

Tong, L. & Rossmann, M. G. (1990). *Acta Cryst.* A**46**, 783–792.

Vagin, A. A., Murshudov, G. N. & Strokopytov, B. V. (1998) *J. Appl. Cryst.* **31**, 98–102.

Vellieux, F. M. D., Hajdu, J., Verlinde, C. L. M. J., Groendijk, H., Read, R. J., Greenhough, T. J., Campbell, J. W., Kalk, K. H., Littlechild, J. A., Watson, H. C. & Hol, W. G. J. (1993). *Proc. Natl Acad. Sci. USA*, **90**, 2355–2359.

Watson, H. C., Duée, E. & Mercer, W. D. (1972). *Nature (London)*, **240**, 130–139.

Zwickl, P., Fabry, S., Bodegain, C., Haas, A. & Hensel, R. (1990). *J. Bacteriol.* **172**, 4329–4338.